

Valence space electron momentum spectroscopy of diborane

Feng Wang^{a,*}, Wenning Pang^b, Ming Huang^b

^a Centre for Molecular Simulation, Swinburne University of Technology, P.O. Box 218, Hawthorn, Melbourne, Vic. 3122, Australia

^b Department of Physics, Polarization Physics Laboratory, Tsinghua University, Beijing 100084, China

Received 1 September 2005; received in revised form 15 January 2006; accepted 16 January 2006

Abstract

A non-classical mechanism of binding in diborane (B_2H_6) is derived quantum-mechanically (B3LYP/6-311++G**) using a dual-space analysis. High-resolution binding-energy spectra of diborane, generated using an outer-valence Green's-function and density-functional theory with a statistical average of model orbital potentials (SAOP), agree satisfactorily with experiment. Electron-correlation energies of diborane produce orbital-based variations in ionization energy in the valence space, but with negligible impact on the shape of only a_g symmetry orbitals as indicated in momentum space. The present work indicates quantitatively that (a) the pair of three-centre banana-shaped $B-H_b-B$ bonds are more accurately described as one diamond-shaped bond with $B-H_b-B-H_b$, (b) all bonds in diborane are electron-deficient including the four equivalent $B-H_t$ bonds, (c) there is no pure $B-B$ bond but contributions from all valence orbitals form an unconventional electron-deficient $B-B$ bond, and (d) only two innermost valence orbitals – $2a_g$ and $2b_{1u}$ – are sp^2 -hybridized and no evidence indicates other valence orbitals of diborane to be hybridized. ©2006 Elsevier B.V. All rights reserved.

Keywords: Electron-momentum spectroscopy; Diborane electronic structure; Dual-space analysis; Density-functional theory; Electron-propagator calculations

1. Introduction

Boranes form an important branch of chemistry—known as boron chemistry, in parallel with carbon chemistry. A “simple” and stable compound of hydrogen and boron – diborane (B_2H_6) – has posed a challenge to the Lewis electron structure or even a molecular-orbital picture [1,2]. Work on boranes led to the award of a Nobel Prize to Brown in 1979 [1]. The major industrial uses [3] are in synthesis in the chemical industry, especially as a catalyst for polymerization of ethene, styrene and butadiene; in the electronics industry to improve crystal growth or to improve electrical properties of pure crystals, and in the production of hard boron coatings on metals and ceramics. It is also used as a rubber vulcanizer and as a component or additive for high-energy fuels [3]. The importance of diborane in structural chemistry is due to its unique chemical structure: it has served as a prototype for hydride bridge [4] and three-centre two-electron ($3c2e$) bonds [5,6]. Chemical reactions of diborane include dissociation [7,8], proton affinity [3], molecular dynamics [9] and van der Waals interactions [10]. Although most authors of theoretical papers on its structure have focused

on isotropic properties such as energetics [11,12], some authors [5] described anisotropic properties of diborane such as the density of molecular charge $\rho(\mathbf{r})$. However, quantitative properties such as orbital electron densities have failed to attract attention. For the latter purpose, distributions of orbital momentum that are quantitatively measured through electron momentum spectra (EMS) [13] have provided direct and quantitative information about Dyson orbitals.

There has been some effort to restore the fundamental chemical concepts from quantum-mechanically obtained results to interpret chemical phenomena [14–19]. The orbital information in momentum space, which traditionally provides a more physical picture has become a complementary source to acquire insight understanding of molecular structures [20–25], mechanisms of chemical bonding [26–32], pathways of chemical reactions [34] and quantitative relationships between structure and activity (QSAR) in computational drug design [35]. Wang [26] introduced a dual-space analysis (DSA) to study molecular structures and chemical bonding, taking advantages of Fourier transform and combining information from both the real (\mathbf{r} -space) and reciprocal spaces (\mathbf{k} -space) [28,27,30–33] to investigate molecular electronic structures. As a component of a collaborative theoretical and experimental attempt to assess orbital cross-sections (momentum distributions) of diborane using electron momen-

* Corresponding author. Tel.: +61 3 9214 5065; fax: +61 3 9214 5075.
E-mail address: fwang@swin.edu.au (F. Wang).

tum spectra, we report here our theoretical results about diborane in its ground electronic state (X^1A_g), using various quantum mechanical models such as conventional calculations of electronic structure (RHF/6-311++G**), density-functional theory (B3LYP/6-311++G**, SAOP/ATVP) and OVGf/6-311++G** models. The RHF/6-311++G** and B3LYP/6-311++G** wave functions are then mapped into momentum space according to an independent-particle approximation and plane wave impulse approximation (PWIA) [13] as orbital MDs.

Discussion of the molecular framework in space and symmetry, which significantly influence the topologies of orbital wave functions, is followed by results from calculations of electronic structure, concentrating on binding-energy spectra and other anisotropic properties. We provide information about electronic structure, and discuss in detail the simulated molecular orbitals in momentum space, in combination with their Dyson orbital densities in coordinate space.

2. Orientation, symmetry and computational details

Molecular geometry and symmetry are an essential part of molecular spectroscopy, molecular orbitals and their interactions. The presence or absence of symmetry has consequences for the appearance of spectra, the relative reactivity of groups, and many other aspects of chemistry, including the way that orbitals and interactions are presented [36,37]. Orbitals within a molecule have a defined relationship to the three-dimensional (3D) structure of the molecule through nuclear positions. The nuclear framework of a molecule might thus affect isotropic properties such as energetics as well as anisotropic properties such as dipole and multipole moments and orbital MDs [27,31]. In diborane with symmetry of point group D_{2h} , two B atoms and four terminal hydrogen atoms (H_t) are orientated in the xz -plane of a Cartesian coordinate system. The origin of this system is located at the midpoint of the B–B bond along the z -axis. The two bridge hydrogen atoms (H_b) connecting the B atom pair, B– H_b –B, locate in the yz -plane, perpendicular to the plane of the other four H atoms, as shown in Fig. 1. The four B– H_t bonds are considered to be equivalent by symmetry, as likewise the four B– H_b bonds. The B atoms, binding hydrogen atoms in both xz - and yz -planes, lie along a principal C_2 -rotational axis, the z -axis.

We optimized the geometry of diborane using the B3LYP/6-311++G** model. Ionization-energy spectra of diborane were

calculated using RHF/6-311++G** and OVGf/6-311++G** employing GAUSSIAN03 [38] and GAMESS02 [39], whereas the SAOP/ATZP model is embedded in the Amsterdam density functional (ADF) suite of programs [40]. The present calculations employ the ATZP basis set, which has been tested [41] as an efficient augmented Slater-type triple-zeta basis set with double polarization, was developed by Chong [42]. All RHF, OVGf and SAOP calculations were performed on the B3LYP/6-311++G** optimized geometry. Complementary to an analysis of orbital electronic structure, we analyzed the distribution of charge density according to the Hirshfeld scheme [43] based on SAOP/ATZP wavefunctions, in which a hypothetical “promolecule” with electron density $\Sigma\rho_B$ is constructed by superposition of spherically symmetric charge densities ρ_B of an isolated atom B. The electron density ρ of the real molecule at each point in space is then distributed over atom A in a ratio $w_A = \rho_A \Sigma\rho_B$ the same as they contribute charge density to that point in the promolecule. The Hirshfeld atomic charge Q_A^H is obtained on subtracting the resulting partial electron density associated with atom A from the corresponding nuclear charge Z as [19,43],

$$Q_A^H = Z - \int w_A(\mathbf{r})\rho(\mathbf{r}) d\mathbf{r} \quad (1)$$

RHF and B3LYP wave functions were used to simulate orbital MDs. With the Born–Oppenheimer approximation and molecular orbital theory (i.e. independent particle approximations), the EMS cross-section for randomly oriented molecules is given in the plane wave impulse approximation (PWIA) by [13,44],

$$\sigma \propto \int d\Omega |\psi_j(\mathbf{k})|^2 \quad (2)$$

which is proportional to the one-electron wavefunction $\psi_j(\mathbf{k})$ in momentum space. The one-electron wavefunction, i.e. Dyson orbitals, in coordinate space, is commonly taken as the HF or Kohn–Sham (KS) orbitals [17,25] under the ground-state configuration-frozen approximation (i.e. neglect of the ionic orbital relaxation). Recent EMS experiments at varied impact energies performed on a multichannel (e,2e) spectrometer indicated that for molecules in the ground electronic state [45] with sufficiently high impact energies [46], valence orbital MDs are independent of the impact energy [47], confirming that the PWIA is a satisfactory approximation under these conditions. The HEMS program [20] was employed in the present work.

3. Results and discussion

3.1. Geometry and orbital ionization spectra

The total energy of B_2H_6 in the ground electronic state (X^1A_g) according to RHF/6-311++G**/B3LYP/6-311++G** and B3LYP/6-311++G**/B3LYP/6-311++G** models was calculated to be -52.827943 and $-53.304498 E_h$, respectively. The bond lengths B– H_t = 1.187 Å and B– H_b = 1.316 Å agree with 1.182 and 1.304 Å, respectively, from an MBPT(2)/6-31G** calculation [8] and with 1.184 and 1.314 Å, respectively, from experimental measurements [6]. The B– H_t bond

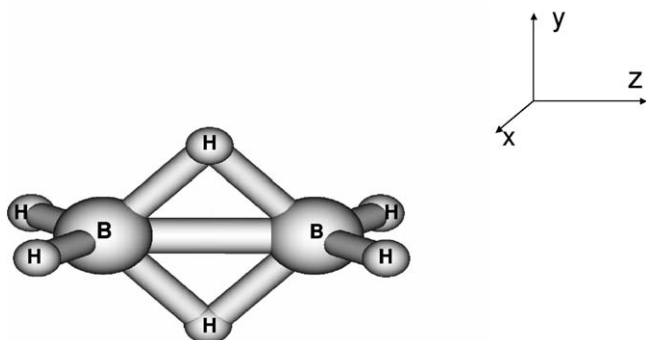


Fig. 1. Diborane (B_2H_6 , D_{2h}) molecule orientation and atom numbering.

Table 1
Comparison of geometry of B₂H₆ ground electronic state (X¹A_g) with other calculations and experiment

Geometry	This work		Other theory		Experiment [6]
	B3LYP/6-311++G**		MBPT(2)/6-31G** [8]	MP2(full)/6-31G* [3]	
B ₍₁₎ –B ₍₂₎ (Å)	1.764		1.752	1.750	–
B ₍₁₎ –H _(t) (Å)	1.187		1.182	1.190	–
B ₍₁₎ –H _(b) (Å)	1.316		1.304	1.308	1.317
H _(t) –B–H _(t) (°)	121.9		121.5	–	–
B ₍₁₎ –B ₍₂₎ –H _(t) (°)	119.1		–	119.2	–
H _(t) –B–H _(b) (°)	109.0		–	–	–
H _(b) –B–H _(b) (°)	95.8		–	–	–
B ₍₁₎ –H _(b) –B ₍₂₎ (°)	84.2		–	83.8	84.4

is slightly shorter than a normal B–H bond, which is 1.188 Å in BH₃ [48], whereas the B–H_b bond in B₂H₆ is elongated apparently, indicating that the B–H_b bonds might be fingerprints of the unique hydride bridge in diborane. According to our B3LYP/6-311++G** calculation, the B–B bond distance is 1.764 Å, in agreement with 1.752 and 1.743 Å given by the MBPT(2)/6-31G** model [8] and experiment [6], respectively. The interbond angle ∠H_tBH_t = 121.87° is consistent with 121.9° and 121.5° from both theory [8] and experiment [6], respectively. The optimized geometry of diborane is summarized in Table 1, with theoretical predictions from other models and experiments. The agreement between results of the present calculation and other theoretical and experimental data indicates that the B3LYP/6-311++G** model is accurate and reliable to predict other molecular properties.

Diborane has too few electron pairs for every connection (nine of them) between atoms to be a conventional two-electron bond. The molecule possesses 16 electrons that form eight molecular orbitals (MOs) including two core MOs and six valence MOs. The valence configuration of the electronic ground state (X¹A_g) given by the B3LYP/6-311++G** model is

$$\dots (2a_g)^2 (2b_{1u})^2 (1b_{2u})^2 (1b_{3u})^2 (3a_g)^2 (1b_{2g})^2$$

The ionization energies of valence orbitals appear in Table 2 with results from photoelectron spectra (PES) measured by Kimura et. al. and their RHF/4-31G calculations [49]. Pole strengths (PS) of our OVGf calculations (all greater than 0.85 [17] for valence orbitals) indicate that an independent-particle

model provides a satisfactory approximation to describe the ionization of diborane.

The computationally expensive calculations with Green's-functions (GF) [50] agree satisfactorily with values from the PES. The GF calculation exhibits competitive accuracy with the binding-energy (ionization energy) spectrum calculated using ΔCI, which takes the energy differences of individual ionic states. The results between the RHF and the ΔCI models [49] indicate a combination of the effects of electron-correlation and orbital relaxation of valence orbitals of diborane. The discrepancies between the outer-valence orbitals produced by two models indicate that the importance of electron-correlation are replaced by orbital relaxation when the hole state moves inwards. The DFT SAOP/ATZP model produces accurate binding-energy spectra of diborane with moderate computational cost, whereas the OVGf/6-311++G** model provides slightly less accurate results that yield a reversed order of orbital pair 1b_{2u} and 1b_{3u}, as seen in Table 2.

3.2. Atom-based electronic structural information of diborane

Diborane is a symmetric (D_{2h}) species with a formally deficient number of electrons, which contributes to its unique molecular electronic structure. Table 3 reports a Hirshfeld [43] charge analysis and components of dipole and multipole moments. These charges, dipole and multipole moments are important anisotropic properties and particularly significant in conform-

Table 2
Molecular orbital energies, symmetry and suggested bonding assignment of B₂H₆ (eV)

MO	This work			Bonding	Bond ^d	Other work			Experiment ^a
	RHF ^b	OVGF ^c	SAOP ^d			RHF (ΔCI) ^e	Bonding ^e	GF [50]	
2a _g	24.16	–	20.77	B(2s, 2p _z)–H _t , B(2s, 2p _z)–H _b	σ ⁺ , S(sp ²)	–	–	22.33	–
2b _{1u}	17.38	17.47(0.87)	16.25	B(2s, 2p _z)–H _t	σ [–] , (S,p)(sp ²)	17.36 (16.14)	B _{2s} [–]	16.21	16.11
1b _{2u}	15.18	15.50(0.90)	15.34	B(2p _y)–H _b	σ, (s,p)	15.16 (14.38)	σ _{B–H_b}	14.49	14.75
1b _{3u}	14.70	15.66(0.91)	14.78	B(2p _x)–H _t	π ⁺ , σ, (S,p)	14.74 (13.75)	π _{B–H₂} ⁺	13.73	13.91
3a _g	14.11	12.24(0.91)	11.94	B(2p _z)–H _t , B(2p _z)–H _b	σ, (S,p)	14.05 (13.17)	σ _{B–B}	13.11	13.30
1b _{2g}	12.83	9.97(0.99)	10.05	B(2p _x)–H _t	π [–] , σ, P	12.75 (11.86)	π _{B–H₂} [–]	11.87	11.89

^a Ref. [49]. ^b This work, RHF/6-311++G**.

^c OVGf/6-311++G** model (pole strength).

^d SAOP/ATZP model.

^e Ref. [49], based on the RHF/4-31G model.

Table 3
Atom-based Hirshfeld charge (Q_A^H) and electric multipole moments of diborane^a(a.u.)

Atom	Q_A^H	μ_x	μ_y	μ_z	q_{xx}	q_{xy}	q_{xz}	q_{yy}	q_{yz}	q_{zz}
B ₍₁₎	1.1960	0.0	0.0	-4.29	-26.29	0.0	0.0	-3.60	0.0	29.88
B ₍₂₎	1.1960	0.0	0.0	4.29	-26.29	0.0	0.0	-3.60	0.0	29.88
H _t	-0.6207	6.93	0.0	-7.87	-1.63	0.0	6.98	3.37	0.0	-1.74
H _t	-0.6207	-6.93	0.0	7.87	-1.63	0.0	6.98	3.37	0.0	-1.74
H _t	-0.6207	6.93	0.0	7.87	-1.63	0.0	-6.98	3.37	0.0	-1.74
H _t	-0.6207	-6.93	0.0	-7.87	-1.63	0.0	-6.98	3.37	0.0	-1.74
H _b	0.0453	0.0	10.28	0.0	1.28	0.0	0.0	0.18	0.0	-1.46
H _b	0.0453	0.0	-10.28	0.0	1.28	0.0	0.0	0.18	0.0	-1.46

^a From SCF equations [19]. The total dipole moment is zero for diborane.

ers and tautomers for which the energetic (isotropic) properties are insensitive to differentiation [32,31,41].

The charges located on component atoms of diborane indicate that the role of the bridge hydrogens in diborane significantly differs from those of the terminal hydrogens: the Hirshfeld charges of the four equivalent terminal hydrogen atoms, H_t, are electron donors, whereas the equivalent bridge hydrogen atoms, H_b, act as electron acceptors. The molecular electrostatic potentials (MEP) given in Fig. 2 illuminate the location of charge in a two-dimensional (2D) plane of diborane. As diborane is such a symmetric molecular species, it possesses no net electric dipole moment, but its components in space indicate significant atom-based charge distributions and polarity in particular directions. For instance, in the *x*- and *z*-directions, the hydrogen atoms behave significantly differently: the terminal hydrogen atoms form two pairs that are polarized significantly in opposite directions. Although the net moment of the terminal hydrogen atoms in the *x*-direction cancels, the resulting charge distributions differ from those of the bridge hydrogens that also exhibit zero μ_x but have no polarization in this direction (see Table 3). The atom-based dipole moments in the *y*-direction, μ_y , are the reverse: the bridge hydrogens, H_bs, are largely polarized in this direction only, but are likewise canceled within the pair, unlike the terminal hydrogens in this direction. The boron atoms are polarized only in the *z*-direction along the B–B “bond”, as indicated by the μ_z dipole moment components being non-zero in

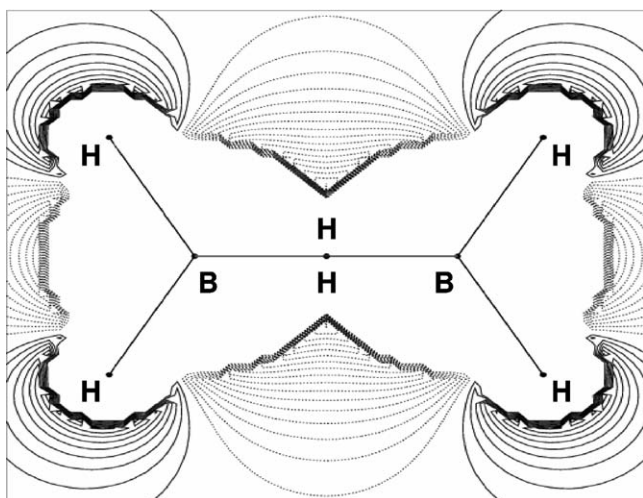


Fig. 2. Molecular electrostatic potential of B₂H₆ in *xz*-plane.

Table 3, which indicates a possible electron-deficient B–B bond described in the next section. Molecular multipole moments and polarizability play important roles in experimental crystal analysis; quadrupole moment components of diborane are thus also given in this table. Quadrupole moments, namely q_{xx} , q_{yy} and q_{zz} indicate the “size” of the species in the pertinent direction; boron atoms in diborane exhibit similar “size” in the *x*- and *z*-directions but are small in the *y*-direction. Such information implies bonding similarities in *x*- and *z*-directions that contrast with the *y*-direction.

All chemical bonds in diborane are electron-deficient, but not all bonds have the population of electrons of equal number. Table 4 presents a population analysis of symmetrized fragment orbitals (SFOs) of diborane based on the SAOP/ATZP calculations. The SFOs are linear combinations of (valence) fragment orbitals (FOs, in diborane, the FOs are atomic orbitals (AOs)), such that the SFOs transform as irreducible representations of the molecular symmetry group [19]. The MO eigenvector coefficients in this basis provide a direct interpretation of the MO according to an orbital theory [40]. The percentages of individual SFOs (AOs) indicate the contribution of AOs of the atoms in the last column of the table into a particular MO given in the first column of the table. The occupation of the AOs for the atoms in the second last column of the table indicates whether the AOs (in the middle column of the table) are occupied or virtual (unoccupied). Therefore, each MO of diborane consists of more than one AOs of different atoms, which are either occupied or virtual. For example, the highest occupied MO (HOMO) 1b_{2g} is dominated by 2p_x AOs of borons (52.98%), 2s, 3s and 1s AOs of H_t atoms (28.59%, 18.74% and -13.78%, respectively), as well as 3d_{xz} and 3p_x AOs of borons (13.41% and -5.05%, respectively). Not all the AOs which form MO 1b_{2g} are occupied: only the 2p_x AOs of borons and the 1s AOs of H_t atoms are occupied with the occupation of 0.33 and 1.00, respectively. As a result, the occupation of MO 1b_{2g} is likely less than 1.33, indicating an electron-deficient MO (the occupation of a normal MO is 2).

Diborane might form nine bonds with four B–H_t bond, four B–H_b bonds and one B–B bond, which share 12 valence electrons. Due to the tetrahedral shape-like boron atoms [51], the boron atoms in diborane was postulated as sp³ hybrids [52]. As a result, if the boron atoms were sp³ hybrid, there should exist only four bonds (for the hydrogens) in a tetrahedral shape and there should not exist any B–B bond in diborane. However, hybridization is more a descriptive hypothesis than a quantitative theory: the 1 + 3 splitting in binding energies of one of

Table 4
Gross population analysis of valence SFO(SAO) in diborane

Orbital	%	SFO(SAO)	Occupation	Atom
1b _{2g}	52.98	2p _x	0.33	B
	28.59	2s	0.00	H _t
	18.74	3s	0.00	H _t
	−13.78	1s	1.00	H _t
	13.41	3d _{xz}	0.00	B
	−5.05	4p _x	0.00	B
3a _g	69.91	1s	1.00	H _t
	14.33	3p _z	0.00	B
	13.11	2p _z	0.33	B
	−10.87	2s	0.00	H _b
	9.33	4p _z	0.00	B
	3.96	1s	1.00	H _b
1b _{3u}	88.81	1s	1.00	H _t
	22.17	2p _x	0.33	B
	−11.16	2s	0.00	H _t
	−5.73	3s	0.00	H _t
1b _{2u}	46.41	2p _y	0.33	B
	32.03	1s	1.00	H _b
	7.73	3s	0.00	H _b
2b _{1u}	113.63	1s	1.00	H _t
	−11.29	2s	0.00	H _t
	−10.71	2p _z	0.33	B
	10.06	3s	0.00	B
	−8.01	4p _z	0.00	B
	5.36	2s	2.00	B
2a _g	49.77	1s	1.00	H _b
	20.49	1s	1.00	H _t
	16.38	2s	2.00	B
	8.00	2p _z	0.33	B

the sp³ hybrid prototypes—methane (CH₄), has been a drawback of the postulation. The tetrahedral structure of methane has been recently proved to stem from the symmetry rather than hybridization [53], which is supported by experiments. The results in Table 4 produced quantitatively provide no evidence that the 2s and three 2p_x, 2p_y and 2p_z orbitals of borons hybridize in sp³ fashion—no single MOs consist of 2p_x, 2p_y and 2p_z orbitals at the same time in this table. Instead, we suggest that the 2s (occupation 2), 2p_x (occupation 0.33) and 2p_z (occupation 0.33) AOs of a boron atom form sp² hybridized orbitals, which is partly supported by HOMO, 1b_{2g} and orbitals 2b_{1u} and 2a_g. HOMO shows the contribution of orbital 3d_{xz} of boron atoms which indicate a hybrid of x and z AOs, whereas MOs 2b_{1u} and 2a_g clearly indicate the mixture of the occupied boron 2s AOs and partially occupied 2p_z boron orbitals. This hybridization in the xz-plane of the terminal BH₂ moieties leaves the boron 2p_y AOs (occupation: 0.33) to bond with the bridge hydrogen atoms in the yz-plane as suggested by Albright and Burdett [54]. Such a hypothesis of an sp² hybrid of boron atoms explains the equivalence of the four B–H_t bonds in the xz-plane, and indicates an electron-deficient B–B bond.

Support of this postulate of sp² hybrid of boron atoms arises from the following evidence. The SFO population analysis in Table 4 indicates that only the innermost valence orbital, 2a_g, and the next innermost valence orbital, 2b_{1u}, show a participation of

boron 2s AO with 16.38% and 5.36% population, respectively; the other valence orbitals of diborane do not exhibit sufficient 2s AO population (less than ±5% of 2s AOs of boron in the table). With regard to the H–B–H angles given in Table 1, the bond angles H_t–B–H_t = 121.9° and B₍₁₎–B₍₂₎–H_t = 119.1° are confirmed by other calculations with MP2 models [3,8]. These angles resemble 120° according to conventional sp² hybrid [51], whereas bond angles B–H_b–B = 84.2° and H_b–B–H_b = 95.8° are near 90° rather than 109° as required for sp³ hybridization [51]. The components of dipole and quadrupole moments (Table 3) indicate that diborane behaves similarly along the x- and z-axes but quite differently in the y-direction. For instance, the individual terminal hydrogens are polarized along both x- and z-axes, whereas the boron atoms are polarized only along the z-axis, which also enhances the polarity of the terminal hydrogens, H_t, in this direction. The boron atoms are not polarized along the y-axis (Table 3). That the dipole components are not zero implies that the three dipole components exhibit a block structure of {μ_y} and {μ_x, μ_z}. The MDs of the innermost valence orbital pair, 2a_g and 2b_{1u}, provide further evidence for such an observation, discussed in the next section.

3.3. Momentum distributions for valence orbitals

Momentum distributions (MDs) of valence orbitals and the corresponding Dyson orbitals (DOs) in coordinate space are shown in Fig. 3. In valence space the MDs indicate that the RHF and B3LYP wave functions obtained employing the same 6-311++G** basis set exhibit no apparent discrepancies in momentum densities, except orbitals 2a_g and 3a_g (Fig. 3(iia) and (via)). That is, the totally symmetric orbitals (a_g) display small variations in the region of small momentum with $p < 0.5$ a.u. between the RHF/6-311++G** and B3LYP/6-311++G** models, as found previously for butane [26]. Such similarities in the Laplacians of the HF and “full CI” Kohn–Sham orbitals were found also for H₂ [16]. As a result, our discussion is based on the B3LYP/6-311++G** model without differentiating the wave functions calculated using the RHF model or the B3LYP models.

The momentum distributions of valence orbital shown in Fig. 3 indicate that the valence orbitals are dominated either by s-like (2a_g and 3a_g) orbitals or by p-like (2b_{1u}, 1b_{2u}, 1b_{3u} and 1b_{2g}) orbitals [29,44], but population analysis based on atoms or fragments (see Table 3) demonstrates that s-electron dominates binding in diborane: there are only two p-electrons in the valence space of 12 electrons in total. Further inspection of the atom-based population analysis, together with the Dyson orbitals, indicates that only the innermost valence orbital, 2a_g, and the HOMO, i.e. the outermost valence orbital, 1b_{2g}, are dominated by the s and p electrons, respectively, as indicated by their orbital MDs. Other valence orbitals are s and p electron mixed orbitals with greater s component, except orbital 1b_{1u} which is dominated by p electrons. The distributions of electron charge in the gaussian-like shaped orbitals, i.e. 2b_{1u}, 1b_{2u}, 1b_{3u} and 1b_{2g}, appear to be p-dominant: they are anti-symmetric with respect to a nodal plane—positive and negative phases are separated by a nodal plane. However, the p-like orbital MDs of these diborane MOs are due to the symmetry in xz-

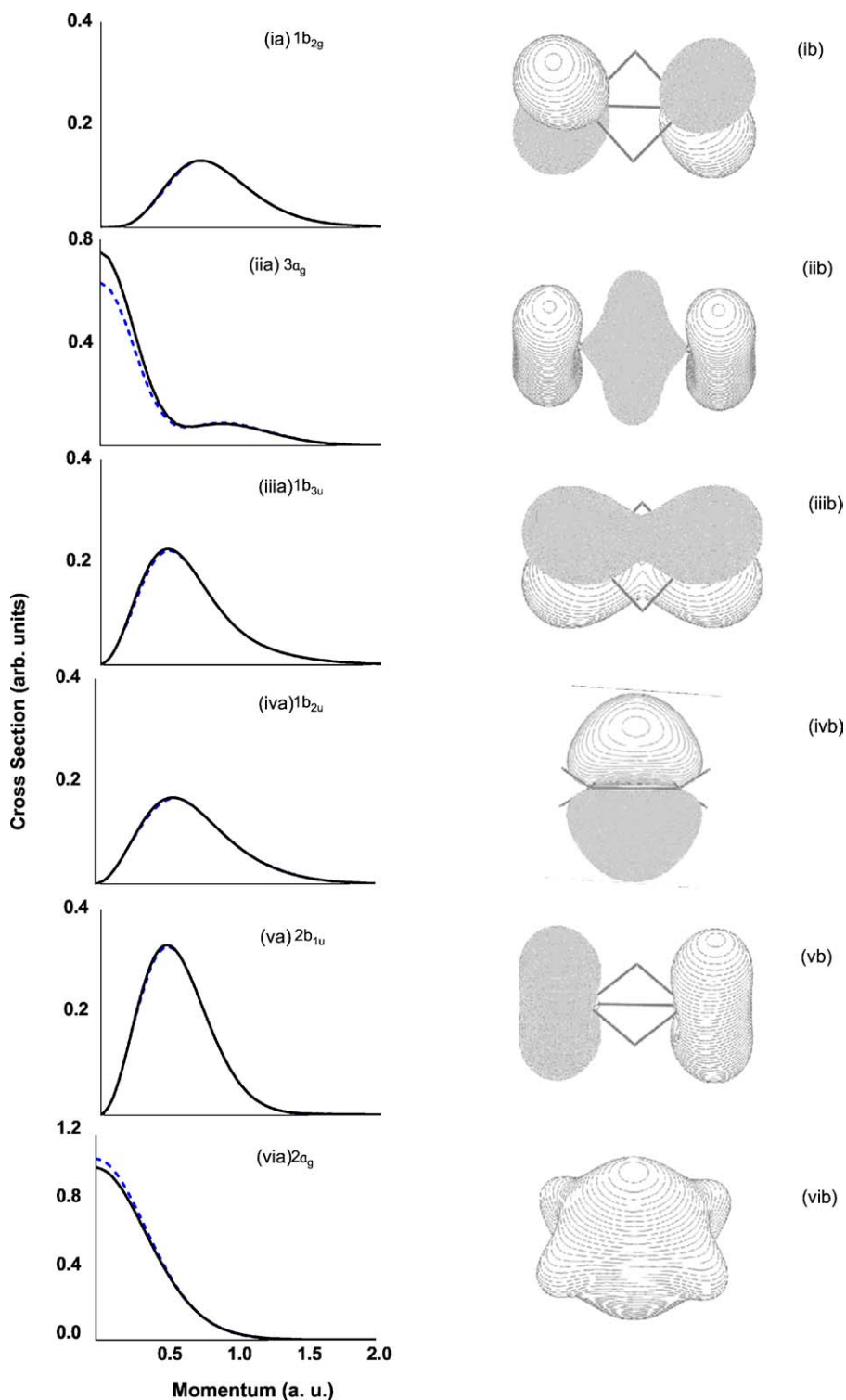


Fig. 3. Valence orbitals of diborane in the ground electronic state (X^1A_g). (a) Orbital momentum distributions (MDs) and (b) electron densities of Dyson orbitals plotted using Molden [55]. Here solid lines represent B3LYP/6-311++G(d,p) model and dotted lines represent RHF/6-311++G(d,p) model.

and xy -planes. The phenomenon of s -electron dominant orbitals exhibiting a gaussian-shaped distribution of orbital momentum is uncommon in atoms and in most molecules [44]. This unique electronic structure of diborane also indicates the importance of obtaining information from both coordinate and momentum space.

The high symmetry of diborane results in its unique non-classical bonding. Based on the gross population of symmetrized fragment orbitals (SFOs) given in Table 4, the valence MOs of diborane are grouped in three classes: the first consists of MOs with only contributions from the terminal hydrogen atoms, H_t , and boron atoms, that is, orbitals $1b_{2g}$ (HOMO), $1b_{3u}$ and $2b_{1u}$.

Only one MO, i.e. orbital $1b_{2u}$ belongs to the second class, of which the orbital involves contributions from the bridge hydrogen atoms, H_b , and both B atoms, whereas orbitals in the third class receive contributions from all atoms in diborane: terminal hydrogen atoms, H_t , bridge hydrogen atoms, H_b and B atoms. Orbitals $3a_g$ (NHOMO) and $2a_g$ belong to this third class. In diborane, the boron atoms are equivalent by symmetry, likewise the four terminal hydrogen atom and the bridge hydrogen pair.

Orbitals in the first class, HOMO $1b_{2g}$, orbitals $1b_{3u}$ and $2b_{1u}$, which are MOs dominated by H_t and borons, represent bonding in the xz -plane. The highest occupied molecular orbital, HOMO $1b_{2g}$, is dominated by the $2p_x$ AOs of borons. A $2p_x$ AO of boron exhibits an occupation number 0.33 for which one electron is shared among the three $2p_x$, $2p_y$ and $2p_z$ AOs of either boron (Table 4). The HOMO also receives large contributions from s AOs of the terminal hydrogen atoms, H_t s, which form a π -like bond of anti-bonding nature (π^-) with the enhancement of four B– H_t bonds shown in Fig. 3(ib). The next MO in this class is orbital $1b_{3u}$, which forms a π -like bond of bonding type π^+ , pairing with the HOMO of π^- . Orbital $1b_{3u}$ receives substantial contributions from the occupied $1s$ AOs of the terminal hydrogen atoms (88.81%) and the $2p_x$ of the borons (22.17%). This orbital ($1b_{3u}$) is dominated by $1s$ contributions even though it exhibits a p-like orbital MDs (Fig. 3(iia) and (iib)). The last orbital in this class, $2b_{1u}$, shown in Fig. 3(va) and (vb), of which the $2p_z$ AOs of borons are responsible, represents sp^2 -hybridized bonding localized on the $BH_2^{(t)}$ moiety, forming a pair of $BH_2^{(t)}$ fragments in the xz -plane, separated by a nodal plane xy , as also suggested in Ref. [54].

Orbitals in the next class are two totally symmetric a_g MOs, which are the only MOs in the valence space of diborane that receive contributions from all atoms, i.e. B, H_t and H_b . The next HOMO (NHOMO), orbital $3a_g$, is a twisted orbital in both xz - and yz -planes, as indicated by the orbital densities in Fig. 3(iib). It is dominated by the singly occupied $1s$ AO of H_t , with small contributions from the singly occupied $1s$ and virtual $2s$ AOs of H_b and a considerable contribution from the occupied $2p_z$ AOs of borons. As the H_t and H_b are in the xz - and yz -planes of diborane, respectively, the two $2p_z$ AOs (occupation number 0.33 each) of borons form a “bond” along the z -axis of type σ . The overlapping region of negative charges in the region of B– H_b –B– H_b are enhanced by the $1s$ AO pair (occupation 1.0 each) of H_b in the yz -plane. The ends of the $2p_z$ – $2p_z$ exhibiting positive charges are each enhanced by the $1s$ AO of H_t , forming a pair of fragments of BH_2 in the xz -plane. Fig. 4 shows 2D orbital density contours (using Molden [55]) of orbital $3a_g$ in xz - (Fig. 4(a)) and yz -planes (Fig. 4(b)); this $3a_g$ orbital “glues” the planes together. The other MO in this class is the innermost valence MO, $2a_g$; beyond the similarities to orbital $3a_g$ as discussed, this MO is an sp^2 -hybrid MO that receives contributions from $2s$ and $2p_z$ AO of borons and $1s$ AOs of H_t and H_b . As a result, it represents a totally symmetric and delocalized “large” π bond (see Fig. 3(via) and (vib)). This orbital, paired with orbital $3a_g$, can be considered as the bonding π^+ and anti-bonding π^- orbital pair.

The last valence orbital of diborane, $1b_{2u}$, differs from all other valence orbitals of diborane: it involves only H_b and boron atoms. The bridge hydrogen atoms locate in the yz -plane so

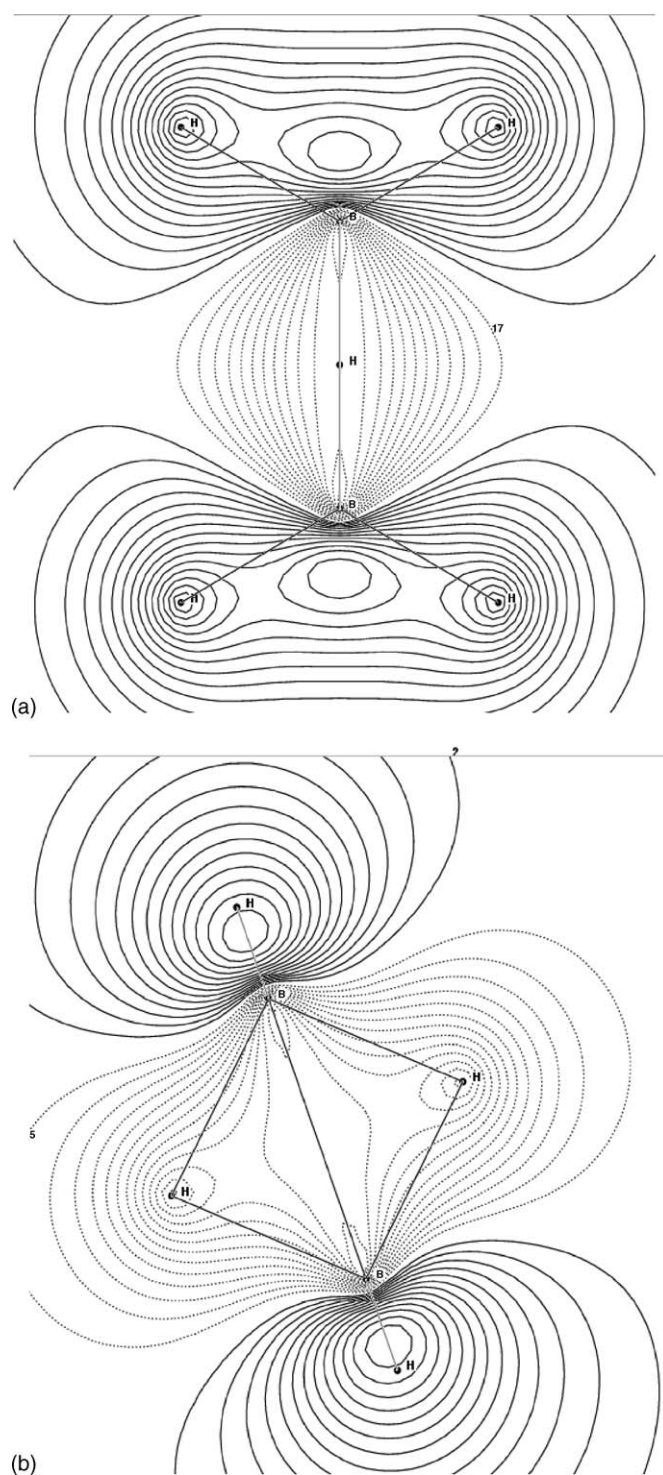


Fig. 4. Two-dimensional contours of electron density for the “glue” orbital $3a_g$ of diborane. (a) The 2D view of H_t –B–B– H_t (xz -plane) and (b) the 2D view of H_b –B–B– H_b (yz -plane). Here solid contours represent positive charges, whereas dotted contours indicate negative charges.

that only the $2p_y$ AO of borons are sterically capable of forming bonds with them. Fig. 3(ivb) demonstrates the orbital densities of the so called “banana” bond [4]. The unoccupied $3s$ AOs of H_b also make noticeable contributions to this MO. The pair of “banana” bonds consists of a positive part and a negative part, which arise from the positive parts of two $2p_y$ AOs

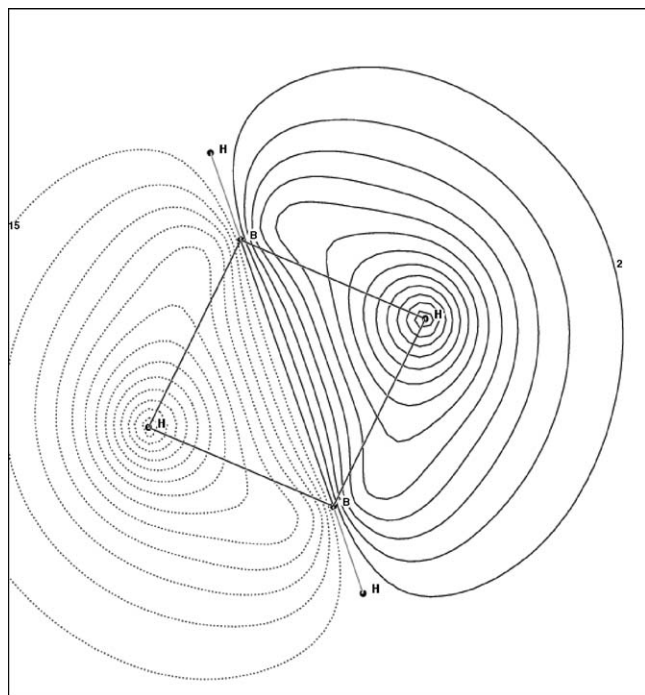


Fig. 5. Two-dimensional contours (yz -plane) of the four-centre diamond bond, i.e. the hydride bridge orbital, $1b_{2u}$, of B_2H_6 . The bonding region of $H_b-B-B-H_b$ is represented in the square formed by a pair of H_b and the borons. Here solid contours represent positive charges, whereas dotted contours indicate negative charges.

of boron plus a $1s$ AO of H_b , and the negative parts of two $2p_y$ AOs of borons plus a $1s$ AO of the other H_b . This pair of “banana” three-centre bonds is actually an integrated “diamond” bond formed among $B-H_b-B-H_b$ atoms. Fig. 5 provides a 2D (yz) view of the electron density of this MO. The nodal plane of this MO separates the positive and negative charges to give a p-like appearance of the orbital MDs shown in Fig. 3(iva).

The electron densities of borons are polarized only along the $B-B$ “bond” (z -axis), as indicated by the non-zero μ_z components of dipole moment in Table 2, reflecting the cylindrical symmetry of diborane along the z -axis. In a boron atom, the three $2p$ AOs are occupied by only one electron yielding an occupation number 0.33. The two $2p_x$ AOs of boron atoms are saturated by two pairs of H_t $1s$ AOs, forming four $B-H_t$ bonds, whereas the pair of $2p_y$ AOs of the boron atoms are “glued” by the bridge hydrogen atoms, H_b $1s$ AOs, forming the positive and negative parts of the $B-H_b-B-H_b$ diamond bond. Because s AOs have no dominant directions in the xyz space (angular momentum quantum number $l = 0$), they add no direction when contributing to bonding but “plumpness” [51]. Only the $2p_z$ AO of each boron atom is polarized through this cylindrical symmetry: the two $2p_z$ AOs of borons form an electron-deficient bond of σ type with their negative parts, whereas the positive parts of $2p_z$ AOs contribute to the $B(H_t)_2$ moieties to enhance their $B-H_t$ bonds. The $2p_y$ AOs of borons contribute to a π type through the $B-H_b-B$ chain. Therefore, “there is still weak σ - and π -bonding interactions between the boron atoms [54]”.

4. Conclusions

The highly symmetric nature (point group D_{2h}) of diborane contributes to its unique non-classical bonding. The pair of boron atoms are equivalent by symmetry, likewise the four terminal hydrogen atoms, and separately the pair of bridge hydrogen atoms. Their role and contribution have been differentiated by properties such as electrostatic potentials and Hirshfeld charges. The distributions of momentum in the valence orbitals seem p electron domination, but further examination of the Dyson orbitals and the symmetrized fragment orbitals revealed that only the innermost ($2a_g$) and outermost ($1b_{2g}$) valence orbitals are genuinely s - and p -dominant orbitals, respectively. The remaining p -like orbitals – $2b_{1u}$, $1b_{2u}$ and $1b_{3u}$ – are s - and p -electron-mixed orbitals; orbitals $2b_{1u}$ and $1b_{2u}$ contain more s character than p character. The orbitally-based electron-correlation energies do not affect orbital wavefunctions significantly in momentum space, as the RHF and B3LYP orbital wavefunctions are almost quantitatively indistinguishable.

Regarding the non-classical bonding of diborane, the $B-H_b-B$ “banana” bond pair dominated by orbital $1b_{2u}$ consists of $2p_y$ AOs of boron and $1s$ AOs of bridge hydrogen atoms. Instead of two three-centre banana bonds, bonding in this region is more accurately described as a four-centre “diamond” bond ($B-H_b-B-H_b$), as each such “banana” contributes to only a half (either positive or negative) of the bond. All bonds in diborane receive contributions from the component hydrogen atoms: no bonds are pure $B-B$ bonds, but there exists a cylindrical, electron-deficient $B-B$ bond [54] with σ - and π -types, that receives contributions from all valence orbitals. No $B-H_t$ bonds are found to be a conventional two-electron bond: all $B-H_t$ bonds are electron-deficient bonds. No quantitative evidence of sp^3 hybridization of boron atoms has been found in the present work, since the $2p_y$ AOs of boron do not mix with other AOs in the bonding by symmetry. The dipole-moment components and quadrupole moments, together with orbital MDs, indicate that sp^2 hybridization in the xz -plane is responsible for only two inner valence orbitals, $2a_g$ and $2b_{1u}$. The sp^2 hybridization is also supported by the related bond angles of near 120° .

Acknowledgments

The Australian Research Council (ARC) supported this work through an ARC International Linkage Award. FW acknowledges the Australian Partnership for Advanced Computing for using the National Supercomputing Facilities. WNP thanks project 10574079 supported by National Natural Science Foundation of China.

References

- [1] H.C. Brown, V. Ramachandran, Adv. Boron Chem. Spec. Pub. R. Soc. Chem. 201 (1979) 151.
- [2] A. Stock, Hydrides of Boron and Silicon, Cornell University Press, Ithaca, NY, 1933.
- [3] L.D. Betowski, M. Enlow, J. Mol. Struct. (Theochem) 638 (2003) 189.
- [4] R.C. Pierce, R.F. Porter, J. Am. Chem. Soc. 95 (1973) 3849.

- [5] R.F.W. Bader, *Atoms in Molecules-A Quantum Theory*, Oxford University Press, 1990.
- [6] J.L. Duncan, J. Harper, *Mol. Phys.* 51 (1984) 371.
- [7] Y.B. Fan, Z.B. Ding, Q.R. Wang, F.G. Tao, *Chem. Phys. Lett.* 328 (2000) 39.
- [8] J.F. Stanton, *Chem. Phys. Lett.* 138 (1987) 525.
- [9] L. Turker, *J. Mol. Struct. (Theochem)* 629 (2003) 279.
- [10] C. Chuang, T.D. Klots, R.S. Ruoff, T. Emilsson, H.S. Gutowsky, *J. Chem. Phys.* 95 (1991) 1552.
- [11] M. Sana, G. Leroy, *J. Mol. Struct. (Theochem)* 187 (1989) 233.
- [12] B. Russcic, C.A. Mayhew, J. Berkowitz, *J. Chem. Phys.* 88 (1988) 5580.
- [13] I. McCarthy, E. Weigold, *Rep. Prog. Phys.* 54 (1991) 789.
- [14] H. Ichikawa, H. Kagawa, C. Kaneko, *Bull. Chem. Soc. Jpn.* 73 (2000) 2001.
- [15] D.L. Cooper, J. Gerratt, M. Raimondi, *J. Mol. Struct. (Theochem)* 229 (1991) 155.
- [16] O.V. Gritsenko, E.J. Baerends, *Theor. Chem. Acc.* 96 (1997) 44.
- [17] O. Dolgounitcheva, V.G. Zakrzewski, J.V. Ortiz, *J. Am. Chem. Soc.* 122 (2000) 12304.
- [18] B. Herrera, O. Dolgounitcheva, V.G. Zakrzewski, A. Toro-Labbe, J.V. Ortiz, *J. Phys. Chem. A* 108 (2004) 11703.
- [19] F.M. Bickelhaupt, E.J. Baerends, in: K.B. Lipkowitz, D.B. Boyd (Eds.), *Reviews in Computational Chemistry*, vol. 15, Wiley-VCH, New York, 2000, pp. 1–86.
- [20] Y. Zheng, J.J. Neville, C.E. Brion, *Science* 270 (1995) 786.
- [21] J.J. Neville, Y. Zheng, C.E. Brion, *J. Am. Chem. Soc.* 118 (1996) 10533.
- [22] W. Adcock, M.J. Brunger, I.E. McCarthy, M.T. Michalewicz, W. von Nesians, W.F. Wang, E. Weigold, D.A. Winkler, *J. Am. Chem. Soc.* 122 (2000) 3892.
- [23] F. Wang, H. Mackenzie-Ross, D.A. Winkler, I.E. McCarthy, L. Campbell, M.J. Brunger, *J. Comput. Chem.* 22 (2001) 1321.
- [24] K. Nixon, F. Wang, L. Campbell, T. Maddern, D. Winkler, R. Gleiter, P. Loeb, E. Weigold, M. Brunger, *J. Phys. B: At. Mol. Opt. Phys.* 36 (2003) 3155.
- [25] P. Duffy, D.P. Chong, M.E. Casida, D.R. Salahub, *Phys. Rev. A* 50 (1994) 4707.
- [26] F. Wang, *J. Phys. Chem. A* 107 (2003) 10199.
- [27] F. Wang, M.T. Downton, *J. Phys. B: At. Mol. Opt. Phys.* 37 (2004) 557.
- [28] M.T. Downton, F. Wang, *Chem. Phys. Lett.* 384 (2004) 144.
- [29] F. Wang, M.J. Brunger, I.E. McCarthy, D.A. Winkler, *Chem. Phys. Lett.* 382 (2003) 217.
- [30] F. Wang, *J. Mol. Struct. (Theochem)* 728 (2005) 31.
- [31] F. Wang, M.T. Downton, N. Kidwani, *J. Theo. Comp. Chem.* 4 (2005) 247.
- [32] S. Saha, F. Wang, C.T. Falzon, M.J. Brunger, *J. Chem. Phys.* 123 (2005) 124315.
- [33] C.T. Falzon, F. Wang, *J. Chem. Phys.* 123 (2005) 214307.
- [34] L. Amat, R. Carbo-Dorca, D.L. Cooper, N.L. Allan, *Chem. Phys. Lett.* 367 (2003) 207.
- [35] E.F. McCoy, M.J. Sykes, *J. Chem. Inf. Comp. Sci.* 43 (2003) 545.
- [36] A. Rauk, *Orbital Interaction Theory of Organic Chemistry*, Wiley-Interscience, New York, 2001.
- [37] R.B. Woodward, R. Hoffmann, *The Conservation of Orbital Symmetry*, Academic Press, New York, USA, 1970.
- [38] M. Frisch, et al., *Gaussian 98, Revision B. 03*, Gaussian Inc., Pittsburgh, MA, 2003.
- [39] M. Schmidt, K. Baldrige, J. Boatz, et al., *J. Comput. Chem.* 14 (1993) 1347.
- [40] E.J. Baerends, J. Autschbach, A. Bérces, et al., *Theoretical Chemistry*, Vrije Universiteit, Amsterdam, The Netherlands, <http://www.scm.com>, ADF version 03.
- [41] C.T. Falzon, D.P. Chong, F. Wang, *J. Comp. Chem.* 27 (2006) 163.
- [42] D.P. Chong, *Mol. Phys.* 103 (2005) 479.
- [43] F.L. Hirshfeld, *Theor. Chim. Acta.* 44 (1977) 129.
- [44] E. Weigold, I. McCarthy, *Electron Momentum Spectroscopy*, Kluwer Academic/Plenum Publishers, New York, 1999.
- [45] M. Takahashi, Y. Khajuria, Y. Udagawa, *Phys. Rev. A* 68 (2003) 042710.
- [46] M. Takahashi, T. Saito, J. Hiraka, Y. Udagawa, *J. Phys. B: At. Mol. Opt. Phys.* 36 (2003) 2539.
- [47] Y. Khajuria, M. Takahashi, Y. Udagawa, *J. Electron Spectrosc. Relat. Phenom.* 133 (2003) 113.
- [48] J.A. Pople, B.T. Luke, M.J. Frisch, J.S. Binkley, *J. Phys. Chem.* 89 (1985) 2198.
- [49] K. Kimura, S. Katsumata, Y. Achiba, T. Yamazaki, S. Iwata, *Handbook of HeI Photoelectron Spectra of Fundamental Organic Molecules*, Japan Scientific Societies Press, Tokyo, 1981.
- [50] L.S. Cederbaum, *J. Phys. B: At. Mol. Phys.* 8 (1975) 290.
- [51] A.L. Companion, *Chemical Bonding*, McGraw-Hill Book Company, New York, 1964 p. 60.
- [52] G.C. Pimentel, R.D. Spratley, *Chemical Bonding*, Holedn-Day Inc., New York, 1969.
- [53] F. Wang, *J. Mol. Struct. (Theochem)* 678 (2004) 105.
- [54] T.A. Albright, J.K. Burdett, *Problems in Molecular Orbital Theory*, Oxford University Press, Oxford, 1992 pp. 161–162.
- [55] G. Schaftenaar, J. Noordik, *J. Comput. Aided Mol. Design* 14 (2000) 123.